Full-Band Monte Carlo simulations of GaAs p-i-n Avalanche PhotoDiodes: What Are the Limits of Nonlocal Impact Ionization Models?

A. Pilotto[1], F. Driussi[1], D. Esseni[1], L. Selmi[2], M. Antonelli[3], F. Arfelli[4,5], G. Biasiol[6], S. Carrato[3], G. Cautero[7,5], D. De Angelis[7], R. H. Menk[7,5,8], C. Nichetti[7,4], T. Steinhartova[4,6], P. Palestri[1]
[1]DPIA, University of Udine, 33100 Udine, Italy. Email: pilotto.alessandro@spes.uniud.it
[2]DIEF, University of Modena and Reggio Emilia, 44100 Modena, Italy.
[3]Department of Engineering and Architecture, University of Trieste, 34128 Trieste, Italy.
[4]Department of Physics, University of Trieste, 34128 Trieste, Italy.
[5]Istituto Nazionale di Fisica Nucleare, INFN Sezione di Trieste, Trieste, 34100, Italy.
[6]IOM CNR, Laboratorio TASC, Area Science Park Basovizza, 34149 Trieste, Italy.
[7]Elettra-Sincrotrone Trieste S.C.p.A, Area Science Park Basovizza, 34149 Trieste, Italy.
[8]Department of Medical Imaging, University of Saskatchewan, Saskatoon, SK S7N 5A2, Canada.

***Abstract*—We present a Full-Band Monte Carlo (FBMC) investigation of impact ionization in GaAs p-i-n Avalanche Photodiodes (APDs). FBMC simulations have been used to compute the gain and the excess noise factor and a new equation has been derived for the extraction of history-dependent impact ionization coefficients from FBMC simulations. Results from FBMC are then compared with the ones of nonlocal history-dependent impact ionization models. We found that at high reverse bias voltages it is important to take into account the fact that secondary carriers are generated with nonzero kinetic energy. Finally, we propose an improved history-dependent model using an energy-dependent mean free path.**

***Index Terms*—Avalanche Photodiodes, Full-Band Monte Carlo, Impact Ionization**

I. INTRODUCTION

Nonlocal History-Dependent (NL-HD) impact ionization models based either on the Dead Space approximation [1] or on effective fields [2]–[4] are often used to estimate the gain (M) and the excess noise factor (F) in avalanche photodiodes (APDs). The strength of NL-HD models lies in their low computational burden, when compared with Monte Carlo simulations, that allows to systematically analyze the trade-offs at the basis of APDs design. The high computational speed, however, comes at the expense of accuracy. In fact, in NL-HD models impact ionization is described at a macroscopic level: the model parameters have to be empirically chosen to fit experimental gain and excess noise factor; furthermore secondary carriers are always generated with zero kinetic energy and can move only in the direction of the applied electric field [1]–[4]. In this paper, we analyze each of these limits of NL-HD models by means of Full-Band Monte Carlo (FBMC) simulations of p-i-n GaAs APDs.

The paper proceeds as follows: the FBMC model, its calibration and the results of FBMC simulations in terms of gain and excess noise factor of thin GaAs p-i-n APDs are presented in Section II. A new equation for the extraction of the history-dependent impact ionization coefficients from FBMC simulations is proposed in Section III and used to analyze the limits of NL-HD models. A new expression for the electron's mean free path to be used in the nonlocal history-dependent model of [4] is also reported in Section III. Finally, conclusions are drawn in Section IV.

This work was supported by Italian MIUR through the PRIN 2015 Project under Grant 2015WMZ5C8.

II. FBMC MODEL

The band structure of GaAs has been computed by using the Local Empirical Pseudopotentials with the form factors from [5]. Spin Orbit Interaction has been included in the calculations as in [6]. The expressions reported in [5] have been used for the carrier-phonon scattering rates, giving results consistent with other FBMCs (not shown). The deformation potentials for acoustic and nonpolar optical phonons have been adjusted in order to match the experimental results for the drift velocities vs. the applied field [7]–[10] (see Fig. 1).

The impact ionization scattering rates are computed from the band structure embracing the Constant Matrix Element approximation [11] and are consistent with other FBMCs, as shown in Fig. 2.

The impact ionization coefficients corresponding to the scattering rates in Fig. 2 are extracted from FBMC simulations under uniform electric field (infinitely long slabs) with two different methods: namely, either as the reciprocal of the average distance $\langle d \rangle$ between consecutive impact ionization events

$$\alpha = \frac{1}{\langle d \rangle}, \tag{1}$$

or by using the expression (valid for electrons)

$$\alpha = \frac{\int_0^{+\infty} SR_{II,e}(W) F_{occ}(W) dW}{v_e \int_0^{+\infty} F_{occ}(W) dW}, \tag{2}$$

where $SR_{II,e}(W)$ and $F_{occ}(W)$ are, respectively, the electron's impact ionization scattering rate and the occupation function as a function of the energy W, while v_e is the drift velocity. Similar equations are used also for the hole impact ionization coefficient β. The two methods are compared in Fig. 3 and give similar results that are in an overall good agreement with experimental data [15], and with the impact ionization coefficients used in the NL-HD model of [4].

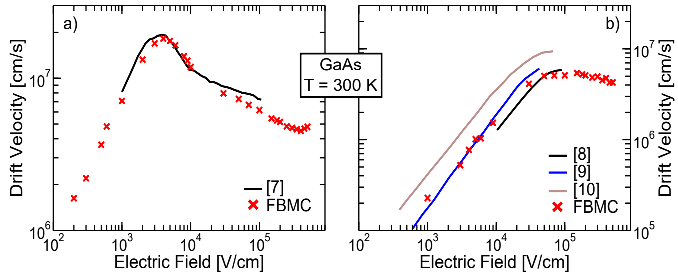

Fig. 1. a) Electron velocity v_e and b) hole velocity v_h versus electric field (E) curves in GaAs at $T = 300$ K. FBMC results (red crosses) are compared with experimental data [7]–[10] (solid lines).

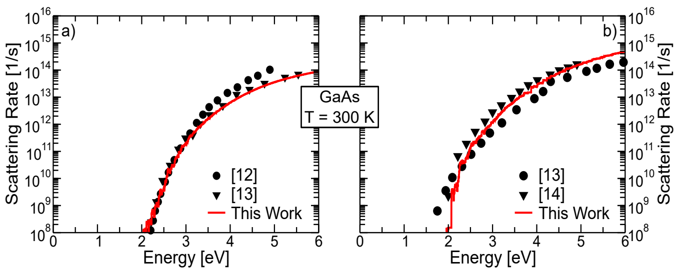

Fig. 2. a) Electron and b) hole impact ionization scattering rates in GaAs as a function of energy. Our results (red lines), obtained by using the Constant Matrix Element approximation [11], are compared with the scattering rates computed by other authors [12]–[14].

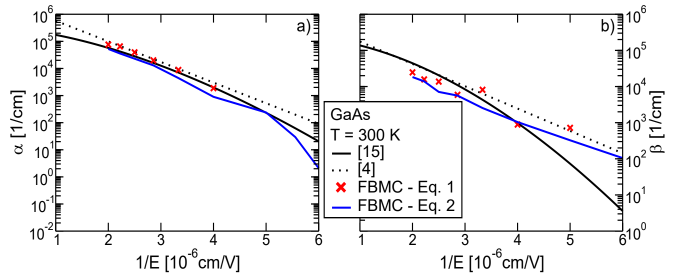

Fig. 3. a) α and b) β versus $1/E$ in GaAs at $T = 300$ K. FBMC (Eq. 1 (red crosses) or Eq. 2 (blue solid)) is compared with experiments [15] (black solid) and with α and β used in [4] (black dotted).

To validate the FBMC transport model, M and F are computed in thin p-i-n diodes by simulating many trials starting from an electron injected at $x = 0$: $M = \langle m \rangle$ and $F = \langle m^2 \rangle / M^2$, with m being the gain obtained in a trial. Figure 4 compares the experimental $M(V_{rev})$ and $F(M)$ curves for GaAs p-i-n diodes of different thicknesses [3] with the results of FBMC. The agreement between experiments and simulations is good with no further parameter adjustments besides the calibration of the phonon deformation potentials carried out to reproduce the $v(E)$ curves of Fig. 1.

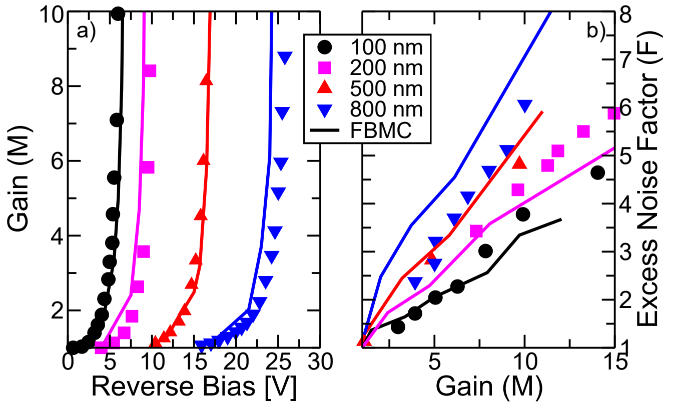

Fig. 4. a) M versus V_{rev} and b) F versus M curves for GaAs p-i-n APDs. FBMC (solid lines) is compared with experiments [3] (symbols). A built-in voltage $V_{bi} = 1.2$ V has been assumed [17].

III. FBMC vs NL-HD Models

In NL-HD models α and β are functions of the generation (x) and the ionization (x') points (see Fig. 5) and they have a nonlocal dependence on the complete electric field profile between x and x'. In other words α and β are not given solely by the local electric field, hence it is also necessary an alternative procedure to extract α and β from simulations with non-uniform electric fields, thus going beyond Eqs. 1 and 2 used for Fig. 3.

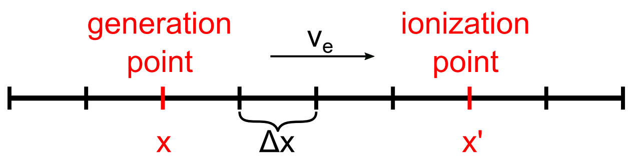

Fig. 5. Discretization of the intrinsic region of a p-i-n diode with a mesh with uniform spacing Δx. x is the point where a carrier is generated, optically or by impact ionization, and x' is the point where it ionizes. Electrons move from left to right with average velocity v_e (while holes move from right to left with average velocity v_h and x and x' are inverted).

To this purpose, we have derived Eq. 3 to extract $\alpha(x|x')$ (and $\beta(x|x')$) from FBMC simulations. In fact, following [2], [4], the electron's impact ionization probability is

$$p(x|x')\Delta x = \frac{\textit{No. of el. gen. in x that ionize in x'} \pm \Delta x/2}{\textit{No. of electrons generated in x}} = \alpha(x|x')\exp\left(-\int_x^{x'} \alpha(x|x''')dx'''\right)\Delta x. \tag{4}$$

With a similar reasoning, one can also find the probability for an electron to ionize before reaching x', namely:

$$p(x|x'' < x') = \frac{\textit{No. of el. gen. in x that ionize before x'}}{\textit{No. of electrons generated in x}} = \int_x^{x'} \alpha(x|x'')\exp\left(-\int_x^{x''} \alpha(x|x''')dx'''\right)dx'' = 1 - \exp\left(-\int_x^{x'} \alpha(x|x'')dx''\right). \tag{5}$$

$$\alpha(x|x') = \frac{\textit{No. of electrons generated in } x \textit{ (by II or a photon) that ionize in } x' \pm \Delta x/2}{\Delta x \cdot (\textit{No. of electrons generated in } x - \textit{No. of electrons generated in } x \textit{ that ionize in } [0, x' - \Delta x/2))} \tag{3}$$

Combining Eqs. 4 and 5, the expression for $\alpha(x|x')$ is found by writing

$$\alpha(x|x') = \frac{p(x|x')}{[1 - p(x|x'' < x')]}, \tag{6}$$

which is equivalent to the proposed Eq. 3. It is worth noting that at the denominator of Eq. 3 we look for all the electrons generated in x that ionize in $[0, x' - \Delta x/2)$, instead of $[x, x' - \Delta x/2)$, to account for those electrons that, due to a scattering event, travel with negative velocity and ionize at points lying before (along the field direction) the location where the carrier was generated.

Sample results are shown in Fig. 6 for an electron generated at $x = 0$ or at $x = 50$ nm. As it can be seen, $\alpha(x|x')$ saturates to a constant value (in the following denoted as α^*) after few tens of nm. The value of α^* differs from the α obtained as a function of the field by using Eqs. 1 and 2. In fact, as explained in [16], α^* is the impact ionization coefficient for an electron which has already traveled over its dead space d_e. Ref. [16] proposes the expression

$$\frac{1}{\alpha} = d_e + \frac{1}{\alpha^*}. \tag{7}$$

Figure 7a compares $\alpha(1/E)$ from Eq. 1 and $\alpha^*(1/E)$ from Eq. 3 when $x' \gg x$ and shows that they can be related by using Eq. 7 with $d_e = W_{th,e}/qE$, where $W_{th,e}$ is the threshold energy for electron's ionization (see Fig. 7b). In Fig. 6b, we notice that at high reverse bias voltages (namely at high gains) $\alpha(x|x') > 0$ also for $x' < x$. In fact, in FBMC secondary carriers are generated with nonzero kinetic energy and in some cases with a velocity going leftward, which is a case neglected by NL-HD models. Such left going electrons can undergo impact ionization events even for $x' < x$.

Figure 8 shows $\beta(x|x')$ for holes extracted from FBMC: also $\beta(x|x')$ saturates to a constant value β^* after few tens of nm. Differently from the case of electrons, the saturation of $\beta(x|x')$ for secondary holes (plot b) takes place after an overshoot that is not present in the NL-HD models. After that overshoot, $\beta(x|x')$ stabilizes to a value independent of x', as long as $x' \ll x$.

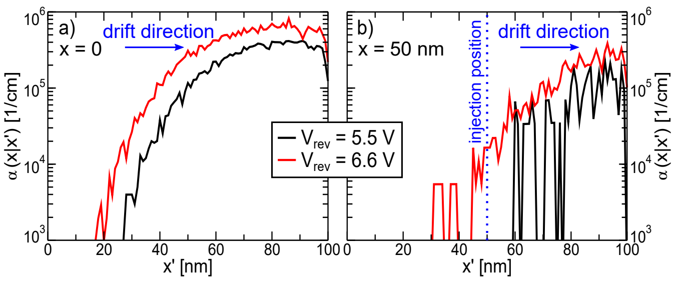

Fig. 6. $\alpha(x|x')$ extracted from FBMC simulations by using Eq. 3 in a 100 nm-thick GaAs p-i-n APD with electron injection from the left side at $V_{rev} = 5.5$ V (black) and $V_{rev} = 6.6$ V (red). a) $x = 0$, b) $x = 50$ nm.

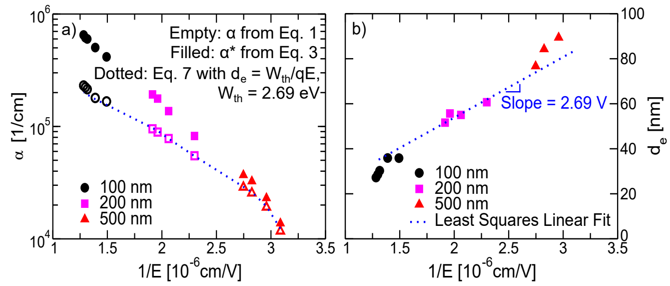

Fig. 7. a) α (empty symbols) and α^* (filled symbols) versus $1/E$ extracted from FBMC simulations of GaAs p-i-n diodes by using Eq. 1 and Eq. 3 (plateau for $x' \gg x$), respectively. b) Electron's dead space d_e versus $1/E$ extracted, point by point, with Eq. 7 from the α and α^* of Fig. 7a with Eq. 7. The blue dotted line in plot b is the least squares linear fit of the d_e values, giving a slope $W_{th,e}/q = 2.69$ V. The same parameter inserted in Eq. 7 gives the blue dotted line in plot a.

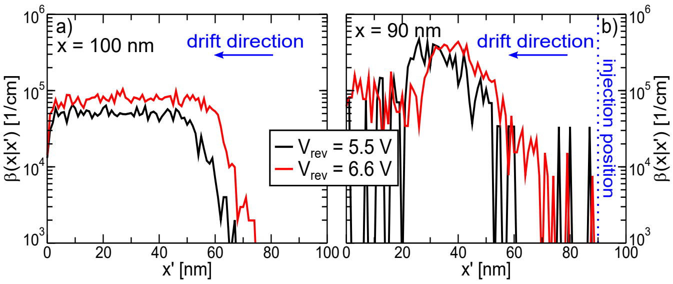

Fig. 8. $\beta(x|x')$ extracted from FBMC simulations by using Eq. 3 in a 100 nm-thick GaAs p-i-n APD with hole injection from the right side at $V_{rev} = 5.5$ V (black) and $V_{rev} = 6.6$ V (red). a) $x = 100$ nm, b) $x = 90$ nm.

Figure 9 compares the $M(V_{rev})$ and $F(V_{rev})$ curves for GaAs p-i-n diodes extracted with FBMC simulations and those obtained with the NL-HD model of [4] by using as input the impact ionization coefficients extracted from the FBMC with Eq. 3. The agreement between the two algorithms for $M(V_{rev})$ is good at low gains and for long diodes. The larger discrepancies at high gains in short devices are due to the fact that the NL-HD model neglects electron impact ionization for $x' < x$ and hole impact ionization for $x' > x$; in fact, such contributions become more relevant as the reverse bias in short devices increases. We also observe that the NL-HD model underestimates $F(V_{rev})$ for short diodes and overestimates $F(V_{rev})$ for long ones.

The NL-HD model we proposed in [4] is based on an energy balance equation with a constant energy relaxation length λ_e. Here we propose the following relation between λ_e and the energy (i.e. the effective field)

$$\lambda_e(x|x') = \frac{A}{B + E_{eff,e}(x|x')}, \tag{8}$$

where the effective field is given by

$$E_{eff,e}(x|x') = \int_x^{x'} \frac{1}{\lambda_e(x|x'')} \frac{dE_C}{dx''} \exp\left(\frac{x'' - x'}{\lambda_e(x|x'')}\right) dx'', \tag{9}$$

and E_C is the conduction band profile. The parameters $A = 1.4142$ V and $B = 1.32 \times 10^5$ V/cm were chosen so that, for each bias point, the $\alpha(0|x')$ computed with the NL-HD model of [4] and $\lambda(x|x')$ from Eq. 8 could reproduce fairly well the $\alpha(0|x')$ extracted from FBMC simulations. Figure 10 compares $\alpha(0|x')$ for a 100 nm thick GaAs p-i-n diode from FBMC and without hole impact ionization, with the NL-HD impact ionization coefficients corresponding to different approximations. The NL-HD results are shown for the Dead Space model [1] (d_e is taken from Fig. 7b) and for the NL-HD model in [4] using the effective fields from Eq. 9 with $\lambda_e = 18$ nm [4] or with λ_e from Eq. 8. Good agreement is obtained between FBMC results and impact ionization coefficients of the NL-HD model in [4] with energy dependent λ_e (Eq. 8). The Dead Space model and the NL-HD model with constant λ_e are instead found to be less accurate.

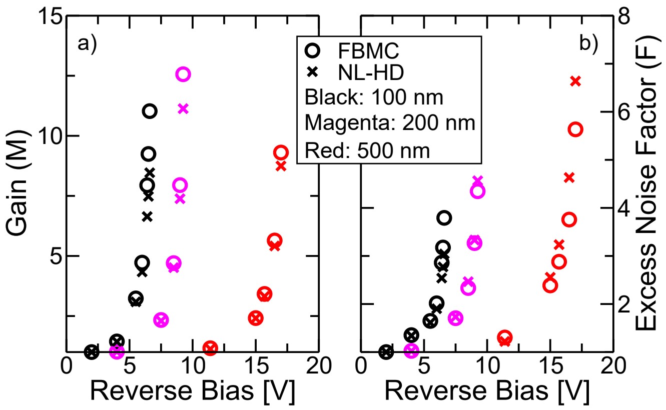

Fig. 9. Comparison between the a) M and b) F versus V_{rev} curves for GaAs p-i-n diodes obtained with the FBMC (circles) or by using the NL-HD model of [4] with $\alpha(x|x')$ and $\beta(x|x')$ extracted from FBMC simulations as inputs (crosses).

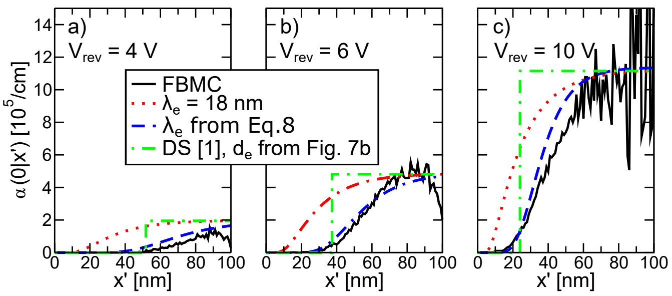

Fig. 10. $\alpha(0|x')$ for a 100 nm-thick GaAs p-i-n diode when hole impact ionization is turned off. FBMC (black solid line) is compared with the NL-HD model for impact ionization in [4] either with $\lambda_e = 18$ nm (red dotted line) or λ_e from Eq. 8 (blue dashed line) and with the Dead Space model (DS) [1], when d_e is taken from Fig. 7b (green dahed-dotted line).

IV. Conclusions

This work identified some major limits of NL-HD models, that mainly stem from the assumption that secondary carriers are generated with zero kinetic energy and can move only in the direction of the electric field, resulting in impact ionization events only at $x' > x$ for electrons ($x' < x$ for holes). The FBMC simulations point out the role of backscattering that may lead to impact ionization at positions preceding the generation point along the field direction, in particular at high gains in short devices. Impact ionization coefficients based on an energy dependent λ_e are in better agreement with the FBMC compared to the Dead Space model or the NL-HD model of [4]. As for the $\beta(x|x')$, however, it seems more difficult to derive an expression similar to Eq. 8 for λ_h in GaAs is not straightforward, essentially because $\beta(x|x')$ saturates to a constant value β^* only after the overshoot region illustrated in Fig. 8.

References

[1] M. M. Hayat, B. E. A. Saleh and M. C. Teich, "Effect of dead space on gain and noise of double-carrier-multiplication avalanche photodiodes," in IEEE Transactions on Electron Devices, vol. 39, no. 3, pp. 546-552, March 1992, doi: 10.1109/16.123476.

[2] R. J. McIntyre, "A new look at impact ionization-Part I: A theory of gain, noise, breakdown probability, and frequency response," in IEEE Transactions on Electron Devices, vol. 46, no. 8, pp. 1623-1631, Aug. 1999, doi: 10.1109/16.777150.

[3] P. Yuan et al., "A new look at impact ionization-Part II: Gain and noise in short avalanche photodiodes," in IEEE Transactions on Electron Devices, vol. 46, no. 8, pp. 1632-1639, Aug. 1999, doi: 10.1109/16.777151.

[4] C. Nichetti et al., "An Improved Nonlocal History-Dependent Model for Gain and Noise in Avalanche Photodiodes Based on Energy Balance Equation," in IEEE Transactions on Electron Devices, vol. 65, no. 5, pp. 1823-1829, May 2018, doi: 10.1109/TED.2018.2817509.

[5] M. V. Fischetti, "Monte Carlo simulation of transport in technologically significant semiconductors of the diamond and zinc-blende structures. I. Homogeneous transport," in IEEE Transactions on Electron Devices, vol. 38, no. 3, pp. 634-649, March 1991, doi: 10.1109/16.75176.

[6] W. Pötz, P. Vogl, "Theory of optical-phonon deformation potentials in tetrahedral semiconductors", in Phys. Rev. B, vol. 24, no. 4, pp. 2025-2037, Aug. 1981, doi: 10.1103/PhysRevB.24.2025.

[7] P. A. Houston, A. G. R. Evans, "Electron drift velocity in n-GaAs at high electric fields," in Solid-State Electronics, vol. 20, no. 3, pp. 197-204, 1977, doi: 10.1016/0038-1101(77)90184-8.

[8] L. H. Holway, S.R. Steele, M. G. Alderstein, Proceedings of the Seventh Biennial Cornell Electrical Engineering Conference (Cornell University Press, Ithaca, NY, 1979), pp. 199–208.

[9] V. L. Dalal, "Hole velocity in p-GaAs,", in Applied Physics Letters, vol. 16, no. 12, pp. 489-491, 1970, doi: 10.1063/1.1653077.

[10] V. L. Dalal, A. B. Dreeben, A. Triano, "Temperature dependence of hole velocity in p-GaAs," in Journal of Applied Physics, vol. 42, no. 7, pp. 2864-2867, 1971, doi: 10.1063/1.1660641.

[11] N. Sano, A. Yoshii, "Impact-ionization model consistent with the band structure of semiconductors," in Journal of Applied Physics, vol. 77, no. 5, pp. 2020-2025, 1995, doi: 10.1063/1.358839.

[12] H. K. Jung, K. Taniguchi, C. Hamaguchi, "Impact ionization model for full band Monte Carlo simulation in GaAs," in Journal of Applied Physics, vol. 79, no. 5, pp. 2473-2480, 1996, doi: 10.1063/1.361176.

[13] D. Harrison, R. A. Abram, S. Brand, "Impact ionization rate calculations in wide band gap semiconductors," in Journal of Applied Physics, vol. 85, no. 12, pp. 8178-8185, 1999, doi: 10.1063/1.370657.

[14] M. V. Fischetti, N. Sano, S. Laux, K. Natori, "Full-band-structure theory of high-field transport and impact ionization of electrons and holes in Ge, Si, GaAs, InAs, and InGaAs," August 2015, doi: 10.13140/RG.2.1.5004.2088.

[15] G. E. Bulman, V. M. Robbins, K. F. Brennan, K. Hess and G. E. Stillman, "Experimental determination of impact ionization coefficients in (100) GaAs," in IEEE Electron Device Letters, vol. 4, no. 6, pp. 181-185, June 1983, doi: 10.1109/EDL.1983.25697.

[16] J. S. Cheong, M. M. Hayat, X. Zhou and J. P. R. David, "Relating the Experimental Ionization Coefficients in Semiconductors to the Nonlocal Ionization Coefficients," in IEEE Transactions on Electron Devices, vol. 62, no. 6, pp. 1946-1952, June 2015, doi: 10.1109/TED.2015.2422789.

[17] S. A. Plimmer, J. P. R. David, D. S. Ong and K. F. Li, "A simple model for avalanche multiplication including deadspace effects," in IEEE Transactions on Electron Devices, vol. 46, no. 4, pp. 769-775, April 1999, doi: 10.1109/16.753712.